AD-A102 042 CASE INST OF TECH CLEVELAND OH DEPT OF MECHANICAL AN--ETC F/G 20/4
THE EFFECT OF BODY FORCES ON THE MOTION AND HEAT TRANSFER OF CO--ETC(U)
DEC 80 S OSTRACH F49620-79-C-0033
UNCLASSIFIED AFOSR-TR-81-0580 NL

END
DATE
FILMED
8 81
DTIC

FILE COPY

AD A102042

13

FINAL SCIENTIFIC REPORT

THE EFFECT OF BODY FORCES ON THE MOTION AND HEAT TRANSFER OF CONFINED FLUIDS

Contract: [redacted] F49620-79-C-0033

by

Simon Ostrach

Approved for public resease; distribution unlimited.

Qualified requestors may obtain additional copies from the Defense Technical Information Service.

Conditions of Reproduction

UNCLASSIFIED

SECURITY CLASSIFICATION OF THIS PAGE (When Data Entered)

REPORT DOCUMENTATION PAGE

READ INSTRUCTIONS BEFORE COMPLETING FORM

1. REPORT NUMBER: AFOSR-TR- 81 -0580	2. GOVT ACCESSION NO.: AD-A102042
3. RECIPIENT'S CATALOG NUMBER	
4. TITLE (and Subtitle): EFFECT OF BODY FORCES ON THE MOTION AND HEAT TRANSFER OF CONFINED FLUIDS	5. TYPE OF REPORT & PERIOD COVERED: FINAL rept. 1 Nov 78 — 31 Oct 80
	6. PERFORMING ORG. REPORT NUMBER
7. AUTHOR(s): SIMON OSTRACH	8. CONTRACT OR GRANT NUMBER(s): F49620-79-C-0033
9. PERFORMING ORGANIZATION NAME AND ADDRESS: CASE WESTERN RESERVE UNIVERSITY, CLEVELAND, OH 44106	10. PROGRAM ELEMENT, PROJECT, TASK AREA & WORK UNIT NUMBERS: 61102F, 2307/A4
11. CONTROLLING OFFICE NAME AND ADDRESS: AIR FORCE OFFICE OF SCIENTIFIC RESEARCH/NA, BUILDING 410, BOLLING AFB DC 20332	12. REPORT DATE: 31 December 1980
	13. NUMBER OF PAGES: 27
14. MONITORING AGENCY NAME & ADDRESS (if different from Controlling Office)	15. SECURITY CLASS. (of this report): UNCLASSIFIED
	15a. DECLASSIFICATION/DOWNGRADING SCHEDULE

16. DISTRIBUTION STATEMENT (of this Report)

Approved for public release; distribution unlimited

17. DISTRIBUTION STATEMENT (of the abstract entered in Block 20, if different from Report)

18. SUPPLEMENTARY NOTES

19. KEY WORDS (Continue on reverse side if necessary and identify by block number)

FREE CONVECTION
CONFINED FLUID
HEAT TRANSFER
BODY FORCES
HYDRODYNAMIC INSTABILITY
THERMAL INSTABILITY

20. ABSTRACT (Continue on reverse side if necessary and identify by block number)

Various modes of flow have been delineated and the nature and extent of these under different conditions have been described. Emphasis has been on confined natural convection configurations. Although specific problems have been treated both experimentally and theoretically, the methods are not now available to predict general flow pattern for a given configuration. This is due to the inherent bidirectional coupling between the boundary layers and the core which is a basic feature of all confined flow problems. Other activity has centered on some new aspects of natural convection with imposed heat flows in more than

DD FORM 1473, 1 JAN 73 EDITION OF 1 NOV 65 IS OBSOLETE

UNCLASSIFIED

SECURITY CLASSIFICATION OF THIS PAGE (When Data Entered)

412

one direction simultaneously and on the interaction of thermal and hydrodynamic instabilities.

Accession For
NTIS GRA&I
DTIC TAB
Unannounced
Justification
By
Distribution/
Availability Codes
Dist | Avail and/or Special
A

FINAL SCIENTIFIC REPORT
THE EFFECT OF BODY FORCES ON THE MOTION AND HEAT TRANSFER
OF CONFINED FLUIDS
Contract: [redacted] F49620-79-C-0033

Dec. 31, 1980

INTRODUCTION

The research program is directed to obtaining detailed information on the fluid motions and transport phenomena that are induced or affected by coupled driving forces. Although in recent years it has been recognized that such phenomena occur naturally in meteorology and oceanography and also in many areas of technology such as crystal growth, materials processing both on Earth and in space, fuels storage and management, solar energy collectors and systems, and nose cone reentry aerodynamics there is relatively little information on them. For some situations of considerable importance no work at all has been done. As a result the various related technologies have developed in an empirical and ad hoc manner so that they rarely perform as anticipated. The research sponsored to date has not only indicated design options to enhance the desirable aspects and to suppress the deleterious ones but has supplied specific information that led to novel approaches to the problems.

The overall program has attempted to study in detail situations of general applicability. Various modes of flow have thereby been delineated and the nature and extent of these under different conditions have been described. Emphasis has been on confined natural convection configurations. Although specific problems have been treated both experimentally and theoretically one essential aspect has not been resolved. That is that there currently does not exist any way of predicting a priori the general flow pattern for a given configuration. This is due to the inherent bidirectional coupling between the boundary layers and the core which is a basic feature of all confined flow problems. As a consequence, every problem has to be treated separately and this has retarded progress. During the past year work has been done to resolve this problem. In addition, work has been done on some new aspects of natural convection with imposed heat flows in more than one direction simultaneously and on the interaction of thermal and hydrodynamic instabilities. The latter two are related to such applications as cooling systems for nuclear reactors and super-conducting magnetics and to nose cone reentry aerodynamics. The details of this work will be presented below.

RESEARCH PROGRESS

I - Natural Convection in Low Aspect Ratio Enclosures

Natural convection phenomena are physically complex and very sensitive to the geometric configuration and imposed boundary conditions. The research on this problem is to determine the nature and extent of flows induced by a body force in an enclosure whose height is much smaller than its length. This configuration which is of considerable technological importance has received little attention to date.

Since the central problem in studying such confined flows is that the flow pattern cannot be predicted even qualitatively a priori a general theoretical approach coupled with an experimental phase was developed to resolve this crucial problem. The unique theoretical approach is to use multiple scaling techniques in the general equations to provide mathematical degrees of freedom for which physical statements can be consistently made throughout the bidirectionally coupled equations. In this way the proper scales (different from the geometric ones) are determined that define any flow sub-structures, such as cells. In other words, the usual dimensionless parameters based on geometric length scales can, at best, lead to qualitative understanding of global flow and isotherm patterns, but they are incapable of indicating any possible sub-structures. The technique is mathematically formal and leads to physically consistent ordering among all relevant equations. To date, a number of different patterns have been determined for low aspect ratio configurations and the conditions for the change from one pattern to another have been delineated. The analyses is to be extended to include wider Prandtl number ranges and other geometric configurations and imposed boundary conditions.

To give guidance for the theoretical work and to obtain much needed information on such flows experiments were also conducted.

There are only a few experimental studies available on low aspect ratio natural convection (Refs. 1,2,3). The flow structures and heat transfer characteristics over wide ranges of the important parameters in the problem are not well understood. The present work is, therefore, intended to give a comprehensive picture on natural convection heat transfer in low aspect ratio enclosures by systematically varying the parameters Ra, Ar and Pr.

A sketch of the present experimental setup is given in Fig. 1. The figure also shows the coordinate system and nomenclature used herein. The hot wall is heated by an electrical heating mat, and the cold wall is cooled by circulating water maintained at a constant temperature. The bottom and top horizontal walls are thermally insulated. The whole setup is carefully enclosed by 5 cm thick fiber glass insulation to minimize heat loss from the system to the surrounding. Comparisons between the electrical inputs and the amounts of heat given to the cooling water have shown that the heat loss to the surroundings when the container is filled with water is less than 4% of the total heat input. Water and aspect ratio of .0625 were tested first. The results of the Nusselt number ($Nu = q/k(T_h - T_c)$, where q is heat transferred per unit width) measurements are presented in Fig. 2. According to the analysis by Bejan and Tien (Ref. 4) all the present data should fall within the intermediate regime, one of the three characteristic flow regimes (the others are the $Ra \rightarrow 0$ regime and the boundary layer regime). The prediction of Nu for the intermediate regime by Bejan and Tien is also shown in Fig. 2 for comparison. Although the agreement is generally good, a close examination of the present data trend reveals that beyond $Ra = 8 \times 10^5$ the Nu values closely follow 1/4 power of Ra, as indicated in Fig. 2. This power of 1/4 of Ra (or $Gr = Ra/Pr$ since Pr is nearly constant) is interesting because it is a characteristic of natural convection heat transfer in the boundary layer along a vertical flat plate, which implies that in the present configuration heat transfer is predominantly determined by boundary layer type flows along the hot and cold walls. Therefore the flows above $Ra = 8 \times 10^5$ in the present work should belong to the boundary layer regime. The boundary layer regime starts earlier than predicted by Bejan and Tien. Another difference between the present data and the analytical result by Bejan and Tien is that in the boundary layer regime the analysis predicts a 1/5 power of Ra instead of the 1/4 power observed in the present work. Validity of the 1/4 power becomes even more apparent if the present data are compared with the available experimental data, as done in Fig. 3. As seen in the figure, the

1/4 power seems to be valid over a wide range of Ra. One characteristic of the boundary layer regime is that Nu becomes independent of aspect ratio as shown by Bejan and Tien (Ref. 4), because heat transfer occurs mainly in the region near the vertical walls. The data taken by Imberger (Ref. 1) for Ar = .019 and water closely follow the curve for Ar = .0625 beyond Ra = 1.5×10^7. We are currently taking the Nu data for Ar = .125 and water to confirm this further. Fig. 3 also shows the results of numerical computations by Lee and Sernas (Ref. 5) for air. Again the calculated values of Nu seem to follow 1/4 power closely. As Fig. 3 shows Nu depends not only on Ra but also on Pr. To investigate this experimentally we have constructed a setup to be used with glycol (Pr = 1.4×10^3), which is similar to the one used by Ostrach et al. (Ref. 3).

The temperature field in the container is studied by a thermocouple probe. Several thermocouples are also imbedded in the bottom and top walls. Fig. 4 shows the temperature distribution along the bottom and top walls for water and Ar = .0625. Except in the regions near the hot and cold walls the temperature variation in the x-direction is relatively small, which is consistent with the aforementioned Nu behavior in the boundary layer regime. Fig. 5 shows temperature distributions in the y-direction at three x locations (all of them are in the core region). All the profiles are found to be similar, and agree with the parallel core solution given by Cormack et al. (Ref. 6) as seen in Fig. 5, which suggests that the flow in the core for Ar = .0625, Ra $< 4.5 \times 10^6$ and water is parallel. A typical isotherm pattern near the hot wall is presented in Fig. 6. This and other similar results show that there is no cellular motion near the vertical walls in the ranges of the parameters studied so far. As seen in Fig. 6, the fluid outside the thermal boundary layer is stably stratified, but the stratification is rather weak (the fluid temperature is nearly uniform over a large part of the core), which is one major reason why the heat transfer rate has the characteristics of heat transfer along a vertical flat plate.

II - Effects of Stabilizing Temperature Gradients on Natural Convection Flows.

Although in many practical situations natural convection in enclosures is often due to heat fluxes imposed simultaneously in more than one direction, very little work has been done on such problems. Also, it is of interest to see if natural convection can be retarded or eliminated by the imposition of a stabilizing gradient. If so, it would be important, for design purposes, to know the magnitude of such stabilizing gradients.

An experimental program to obtain such quantitative information has been completed. The enclosure was a square, the Prandtl number was 89,000, and the horizontal Rayleigh number ranged from 2.29×10^4 to 5.99×10^4. Stabilizing gradients up to a ratio of the horizontal to vertical Rayleigh numbers of 6. Significant flow retardation was obtained and the details of the velocity and temperature fields were obtained as functions of the conditions. A paper has been prepared (Ref. 7) which describes the work in detail.

III - Natural Convection in a Water Layer with Localized Heating from Below.

Natural convection flows induced by localized heating at the base of an open tank containing water was studied experimentally. This was done to obtain some physical insight into the flow phenomena involved in deep-water waste heat disposal as well in other diverse applications as home heating, thermal pollution, and nuclear reactor design.

The flow is specified by four dimensionless parameters: Ar(aspect ratio, depth of water layer/half width), Hr(heater ratio, radius of heat source/half width of the tank), Pr(Prandtl number), Gr(Grashof number). The aspect ratios for the present experiments were .05, .24 and .37. The heater ratio was fixed at .17. Pr was about 7. The Grashof numbers were of the order of 10^4 - 10^7. The Grashof number was varied by changing the depth of the water layer and the heat source temperature. The ambient conditions (room temperature and humidity) were kept nearly constant. This work is different from the case of heating the whole lower plate. For the latter case, only when the Rayleigh number exceeds a critical value, the layer becomes unstable and the motion strats. For the case of localized heating from below once heating starts, the motion starts immediately, because of the horizontal thermal gradient.

The convective flows were visualized by using an electrochemical technique and a conventional light beam/dust particle method. The temperature distribution in the fluid were measured by a thermocouple probe. When the water layer reached a steady state, it was then mixed uniformly to measure the bulk mean fluid temperature, which is proportional to the Nusselt number Nu (the dimensionless heat transfer rate from the heater to the fluid). Many photographs were taken at several locations in the fluid under various experimental conditions, from which the flow structure were analyzed.

The results of temperature distribution measurements show that natural convection significantly alters the distribution as Ar increases. Two rotating cells (one near the heating zone and the other near the side wall) were found when Ar = .24, .37 and Gr of the order 10^6 - 10^7, but no cells were observed for Ar = .05. Nu was found to be related to Fr and Ar as

$$Nu \, \alpha \, Gr^{.5} \, Ar^{-1.25}$$

This is in agreement with the numerical results of Torrance and Rockett [8] in which Nu is proportional to $Gr^{.5}$ for Ar = 1. The above expression shows that for fixed Gr, Nu decreases with Ar, and also the dependance of Nu on Gr is strong (the power .5) for natural convection. Nonuniformity of temperature distributions decreases with Ar. Compared to the conduction values it can be said that the effect of convection becomes more important as Ar increases.

The present work has qualitatively demonstrated that an introduction of hot effluents deep in a lake could at low Froude numbers induce a thermal convection capable of generating strong mixing flows. These induced flows could be beneficial for dissipating waste heat.

A paper, Ref. 9, has been prepared for presentation and publication.

IV. Combined Thermal and Hydrodynamic Instabilities

In this project boundary layer flows along a heated concave wall are studied experimentally. Under certain conditions the heating and concave wall curvature cause thermal instability and hydrodynamic instability (Görtler instability), respectively. Interactions of those instabilities are our main interest. The experimental setup for this experiment is sketched in Fig. 7. A concave channel test section is attached to a low-speed wind tunnel. The test section is 26.7 cm wide, 5.3 cm high and 53.3 cm long. The bottom plate is made of aluminum and bent carefully to obtain a uniform curvature. Two radii of curvature (50 and 75 cm) have been chosen to obtain the proper Grashof (Gr) and Görtler (G) number ranges. Since not much information is available concerning the pure Görtler instability, we have decided first to conduct some experiments without heating the bottom plate. The flow structure is studied by a flow visualization technique (smoke injection) and by a hot-wire probe. Some of the results obtained thus far are given below.

The mean velocity distributions in the spanwise direction (Z direction in Fig. 7) measured at five X locations and at various distances from the wall are presented in Figs. 8-12. Since the Görtler number is defined as $G = (U\delta/\nu)\sqrt{\delta/R}$ (δ; boundary layer thickness, R; radius of curvature), it increases with X, which means the flow becomes more unstable with increasing X. As seen in Figs. 8-12, the flow is already slightly disturbed at the smallest X location X = 7 cm (corresponding to G = 36.5), and the disturbance increases sharply as we go further downstream, clearly indicating the existence of the Görtler instability. Fig. 13 shows the change of the calculated standard deviation of the mean velocity variation in the Z-direction at the y-location corresponding to $U/V_0 = .7$. The figure shows that the disturbance level increases sharply beyond G = 50. The velocity profile in the boundary layer at X = 7 cm is very close to the flat plate Blasius profile (Fig. 14), but at X = 39.5 cm (G = 134) the profile is severely altered (Fig. 15).

The experimental data are presently being analyzed in order to show the effect of the Görtler instability on the boundary layer structure in an appropriate quantitative way. We plan to study the effects of the free stream velocity and wall curvature. On the above results, and then to study the combined effect of thermal and hydrodynamic instability.

PUBLICATIONS

In addition to those papers presented under References as numbers 3, 7, and 9 the following was also prepared during the past year.

Ostrach, S. and Hantman, R.: Natural Convection Inside a Horizontal Cylinder, presented at the 88th AIChE National Meeting June 1980 and to be published in Chemical Engineering Communications, vol. 7, 1981.

REFERENCES

1. Imberger, J., "Natural Convection in a Shallow Cavity with Differentially Heated End Walls", Journal of Fluid Mechanics, Vol. 65, Part 2, 1974.

2. Al-Homoud, A.A., "Experimental Study of High Rayleigh Number Convection in Horizontal Cavity with Different End Wall Temperatures", M.S. Thesis, College of Engineering, University of Colorado, 1979.

3. Ostrach, S., Loka, R.R. and Kumar, A., "Natural Convection in Low Aspect Ratio Rectangular Enclosures", Natural Convection in Enclosures, HTD-8, ASME, 1980.

4. Bejan, A. and Tien, C.L., "Laminar Natural Convection Heat Transfer in a Horizontal Cavity with Different End Temperatures", Journal of Heat Transfer, Trans. ASME, Vol. 100, 1978.

5. Lee, E.I. and Sernas, V., "Numerical Study of Heat Transfer in Rectangular Air Enclosures of Aspect Less Than One", ASME Paper No. 80-WA/HT-43, 1980.

6. Cormack, D.E., Leal, L.G. and Imberger, J., "Natural Convection in a Shallow Cavity with Differentially Heated End Walls, Part 1, Asymptotic Theory", Journal of Fluid Mechanics, Vol. 65, Part 2, 1974.

7. Fu, B.-I. and Ostrach, S.: The Effects of Stabilizing Thermal Gradients on Natural Convection Flows in a Square Enclosure, to be presented at the 20th National Heat Transfer Conference and published in the Jour. of Heat Transfer, 1980.

8. Torrance, K.E. and Rockett, J.A.: Numerical Study of Natural Convection in Enclosures with Localized Heating from Below, Creeping Flow to the Onset of Laminar Instability, J. Fluid Mech., vol 36, 1969.

9. Kamotani, Y., Wang, L.W. and Ostrach, S.: Natural Convection in a Water Layer with Localized Heating from Below, Submitted for presentation

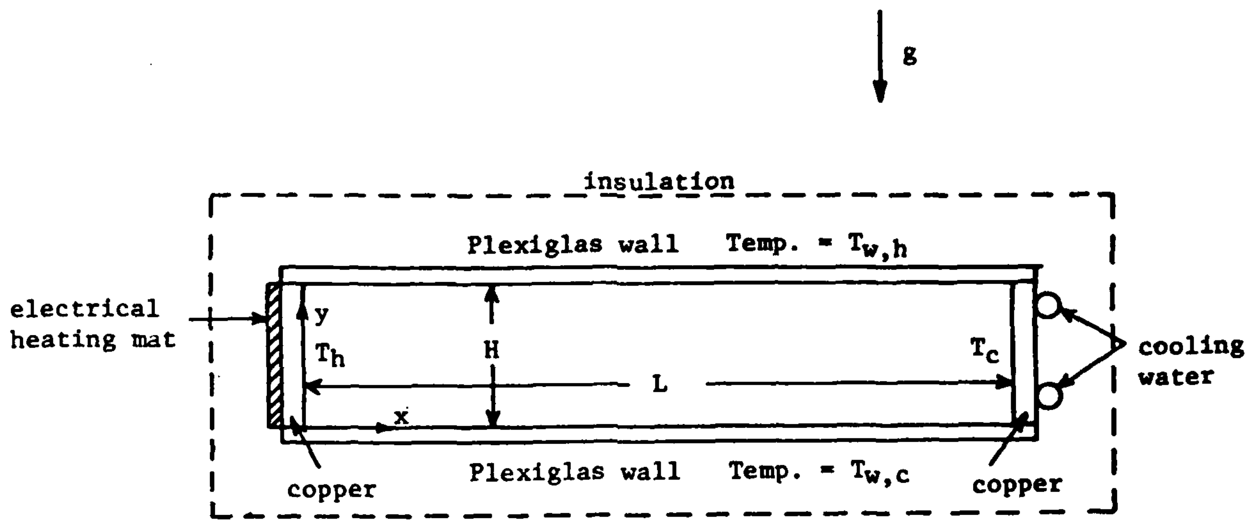

L = 40.6 cm

H = variable

Ar = H/L

Ra = $g\beta \Delta T H^3/\nu\alpha$

Pr = ν/α

$\Delta T = T_h - T_c$

ν = kinematic viscosity

α = thermal diffusivity

β = volumetric expansion coefficient

Figure 1. Experimental Setup

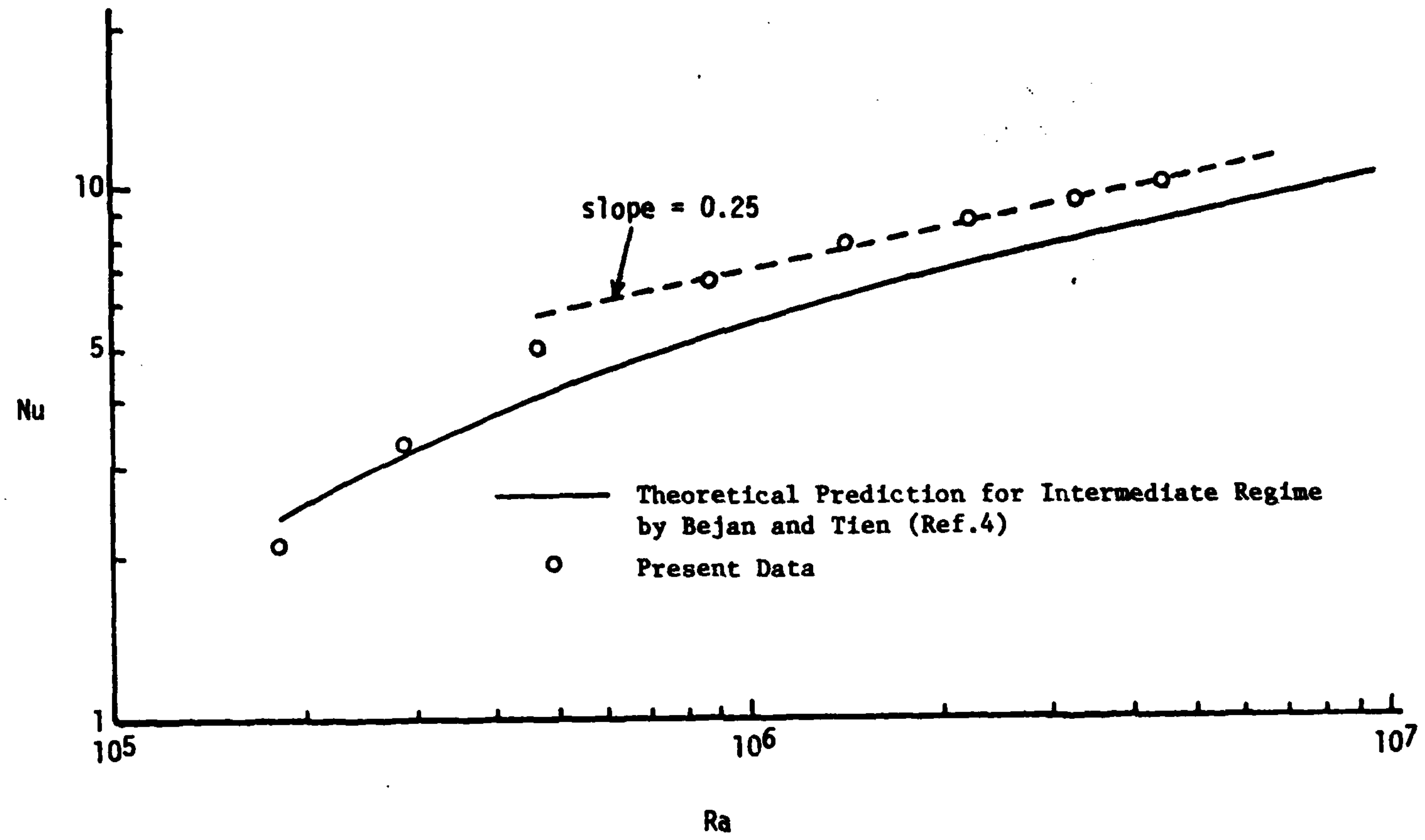

Figure 2. Nu vs. Ra

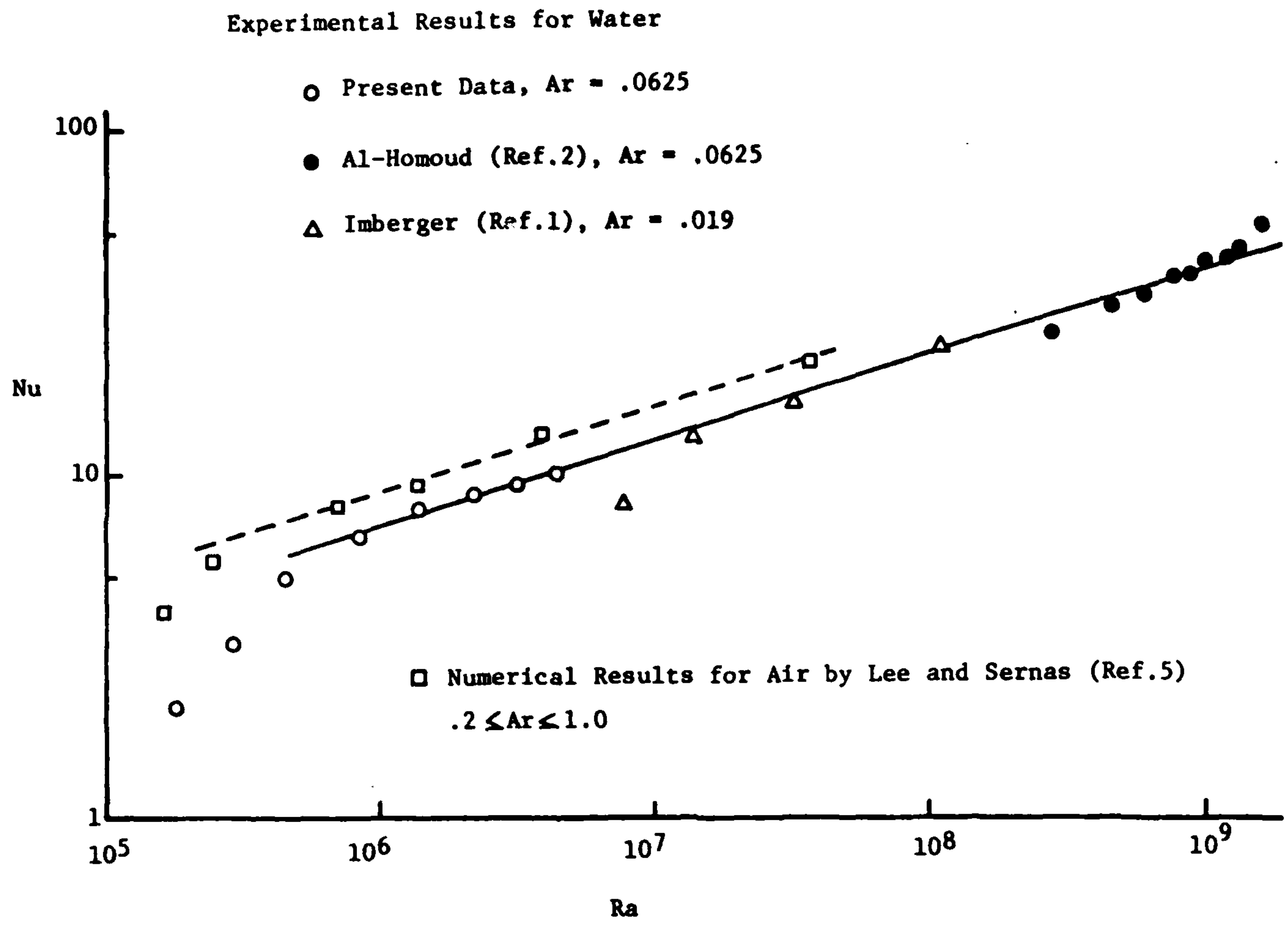

Figure 3. Comparison of Nu among Available Data

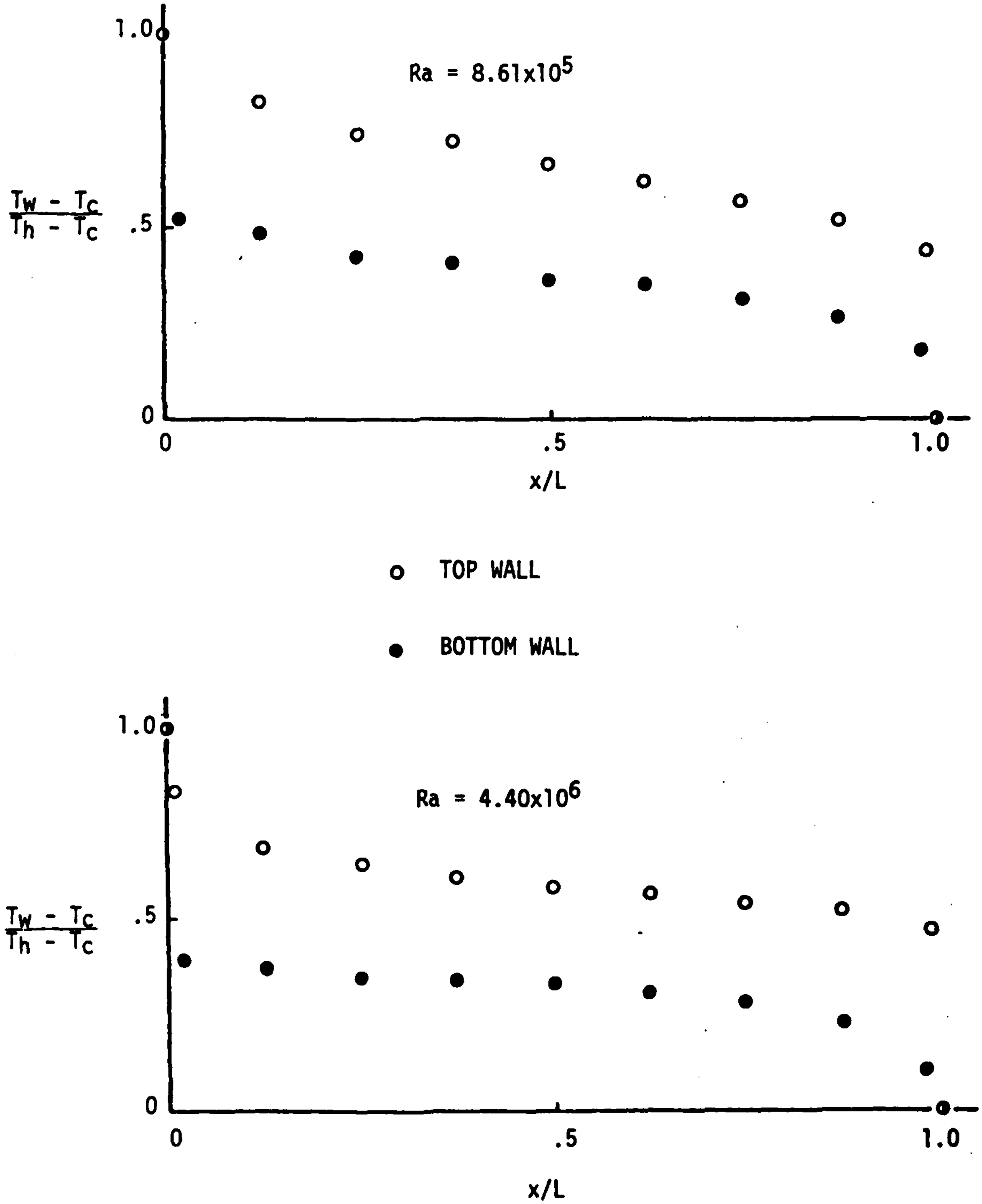

Figure 4. Temperature Distributions along Horizontal Walls

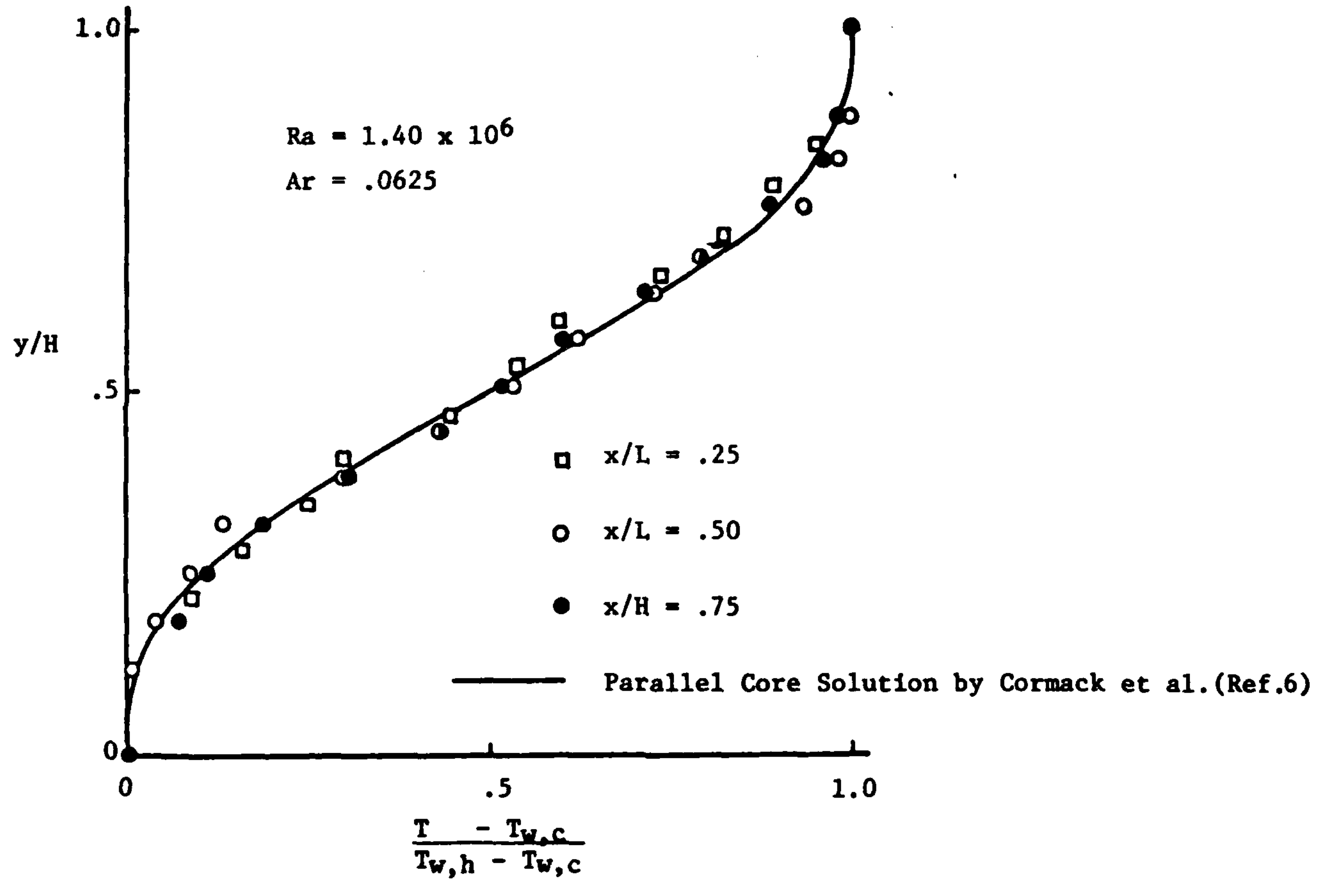

Figure 5. Temperature Distributions in the Core Region

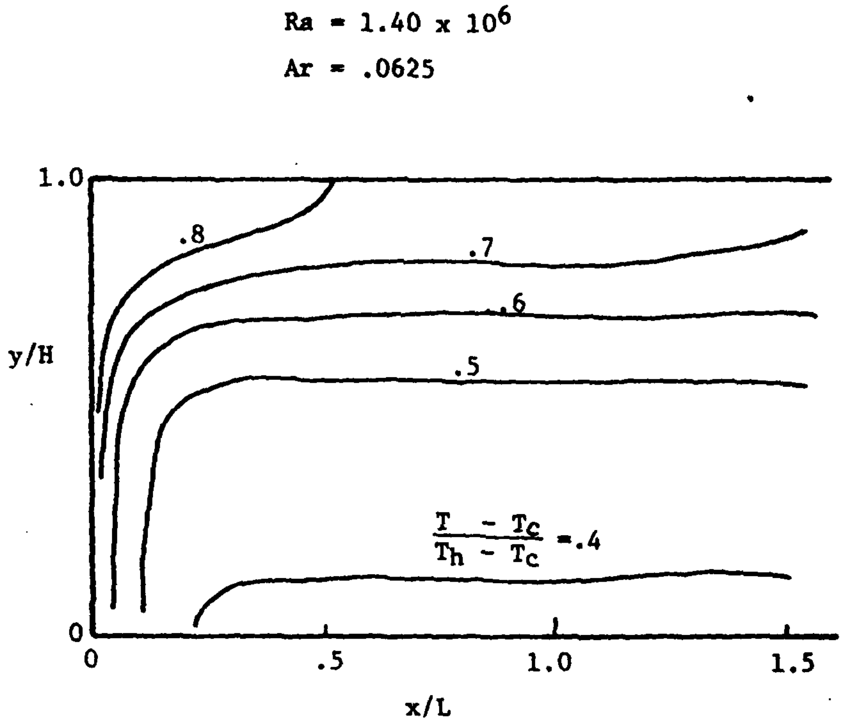

Figure 6. Isotherms near Hot Wall

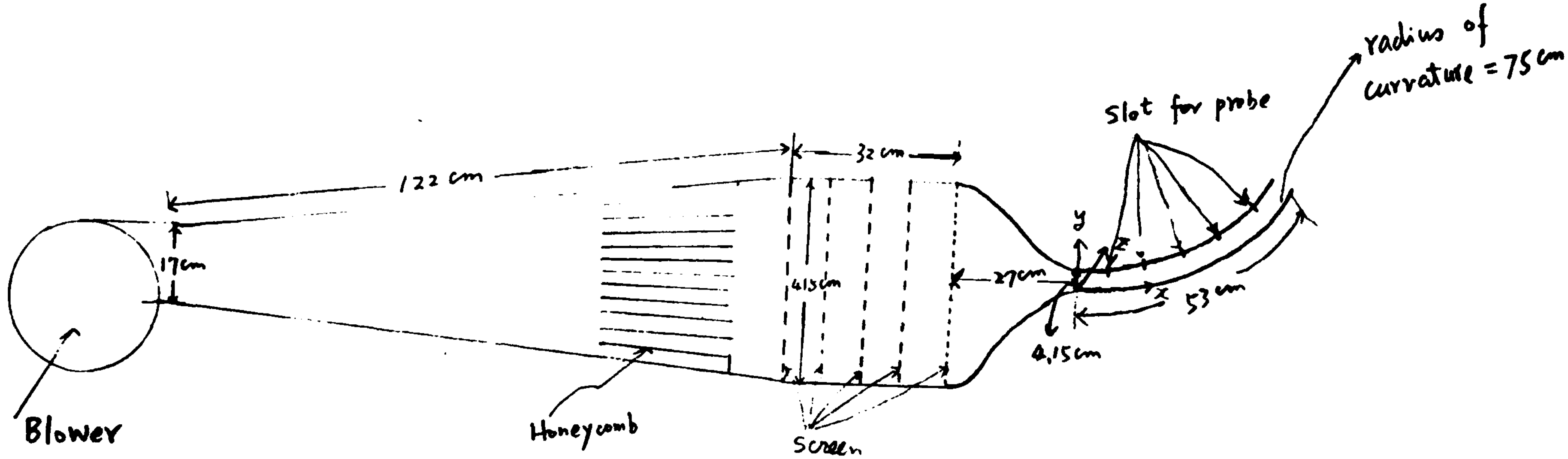

Fig. 7 EXPERIMENTAL APPARATUS

K-Σ 461510

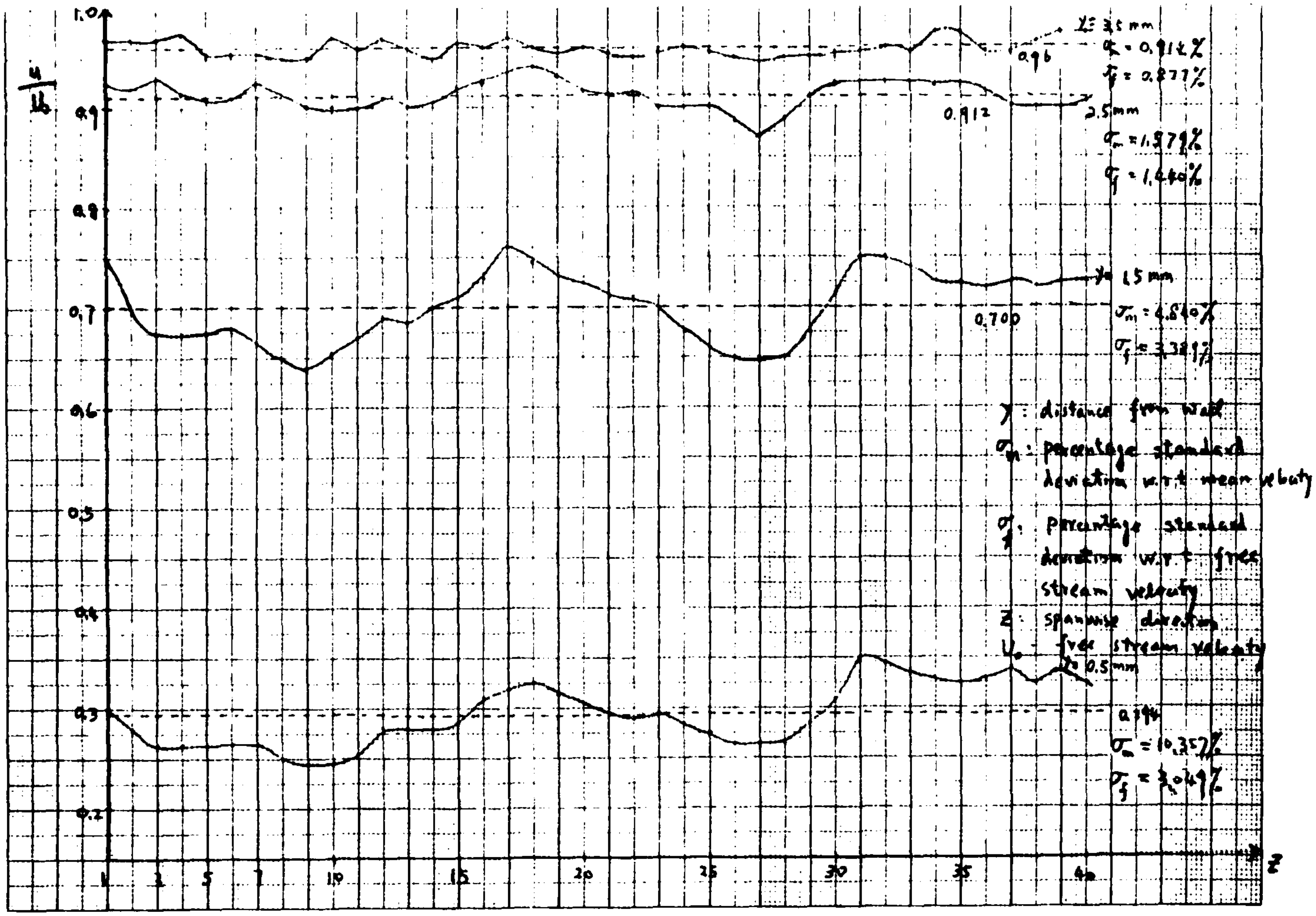

7cm from leading edge, 1st slot $G \simeq 36.5$. $\delta \simeq 3.06$ mm $U_0 = 276$ cm/sec, each step in $Z = 0.25$cm.

Fig. 8 Mean Velocity Distribution at $x = 7$ cm

461510

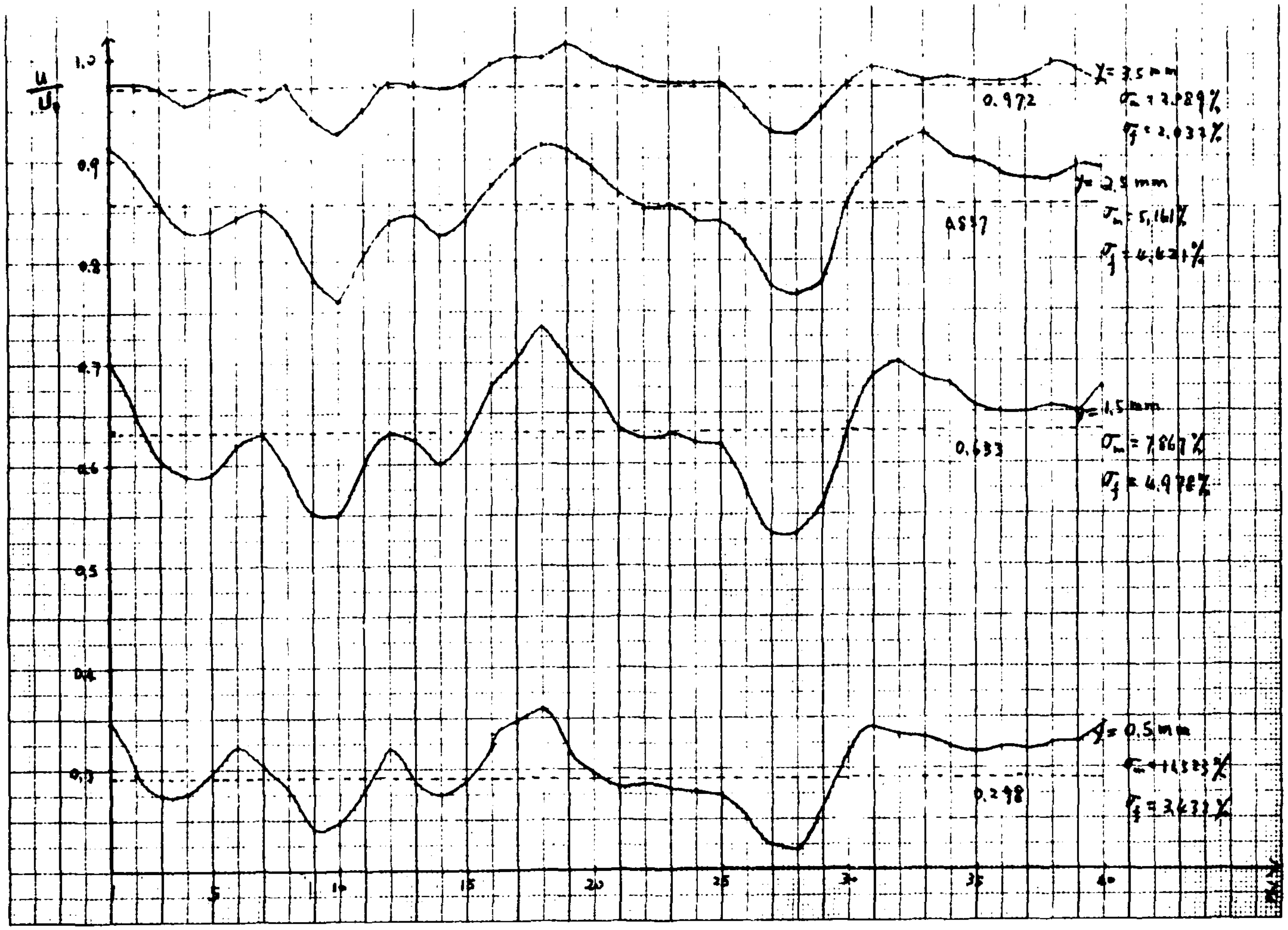

14.5 cm from leading edge, Second slit, G = 63, δ = 4.40 mm U_0 = 276 cm/sec.

Fig. 9 Mean Velocity Distribution at x = 14.5 cm

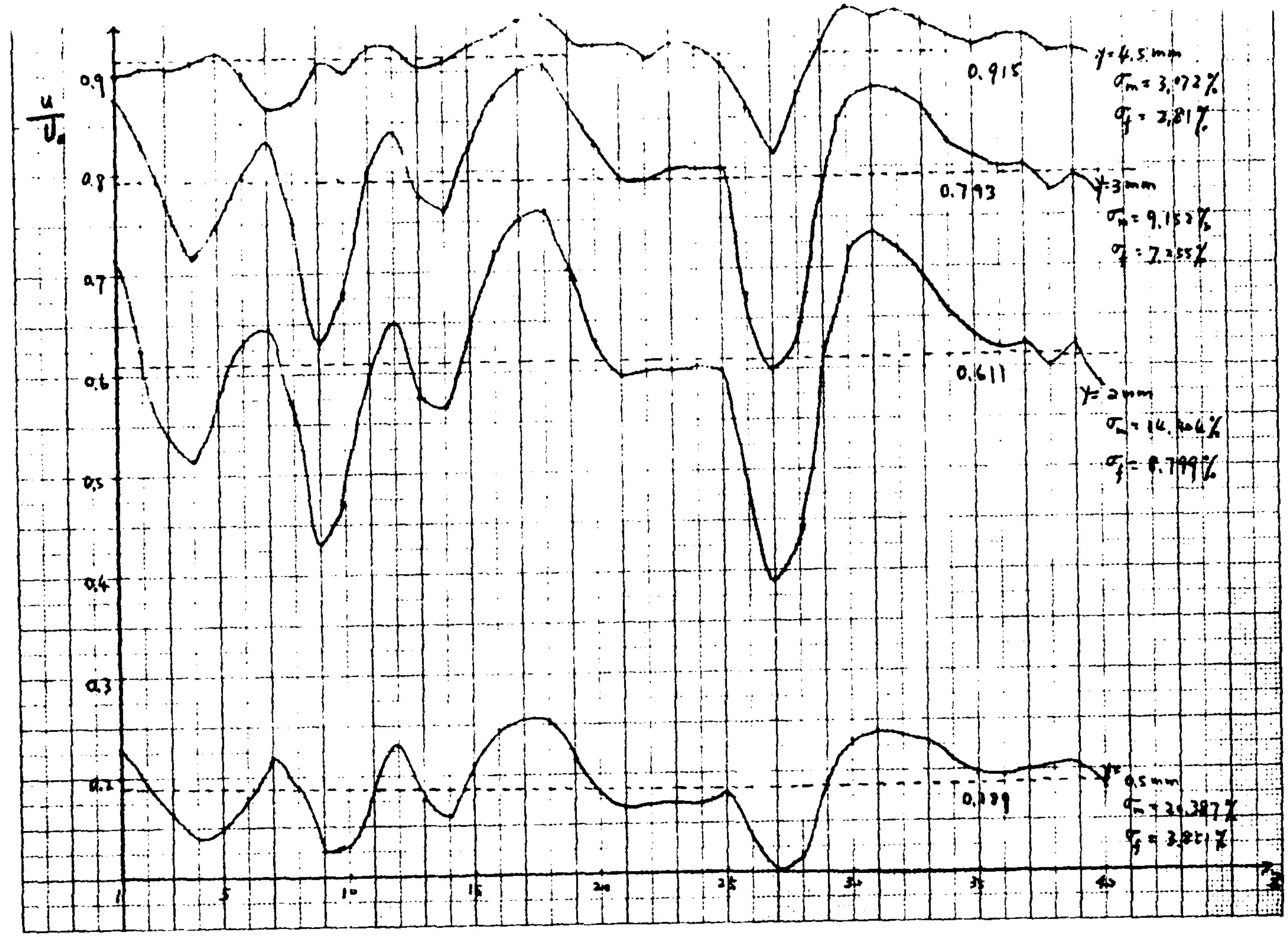

22 cm from leading edge Third slit , $G \approx 8$, $\delta = 5.42$ cm , $U_0 = 276$ cm/sec , each step in $z = 0.25$ cm

Fig. 10 Mean Velocity Distribution at $x = 22$ cm

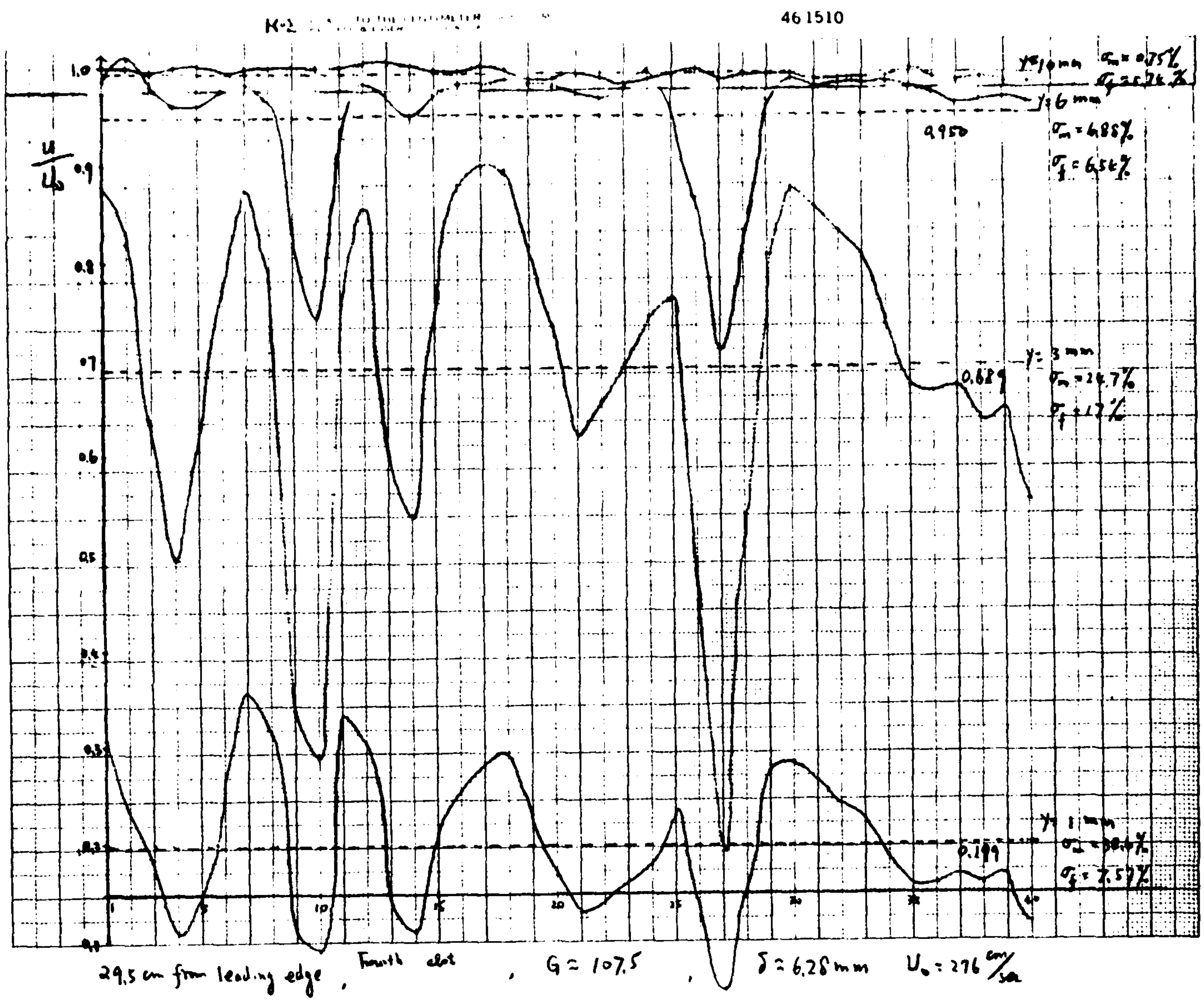

29.5 cm from leading edge, Fourth slot, $G = 107.5$, $\delta = 6.28$ mm $U_0 = 276$ cm/sec

Fig. 11 Mean Velocity Distribution at $x = 29.5$ cm

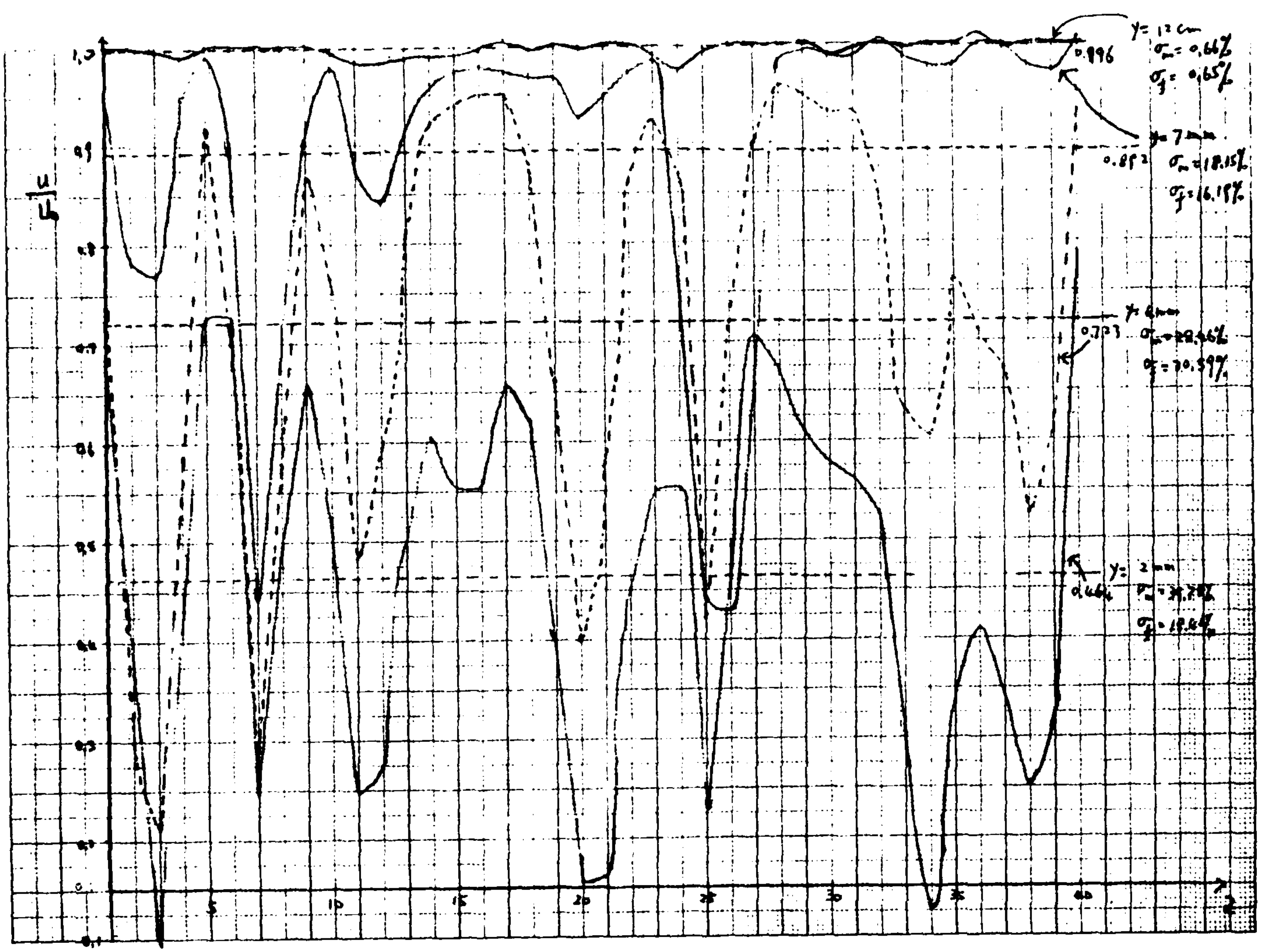

39.5 cm from leading edge. Fifth slot, $\delta = 7.27$ mm, $G = 133.8$, $U_0 = 276$ cm/sec

Fig. 12 Mean Velocity Distribution at $x = 39.5$ cm

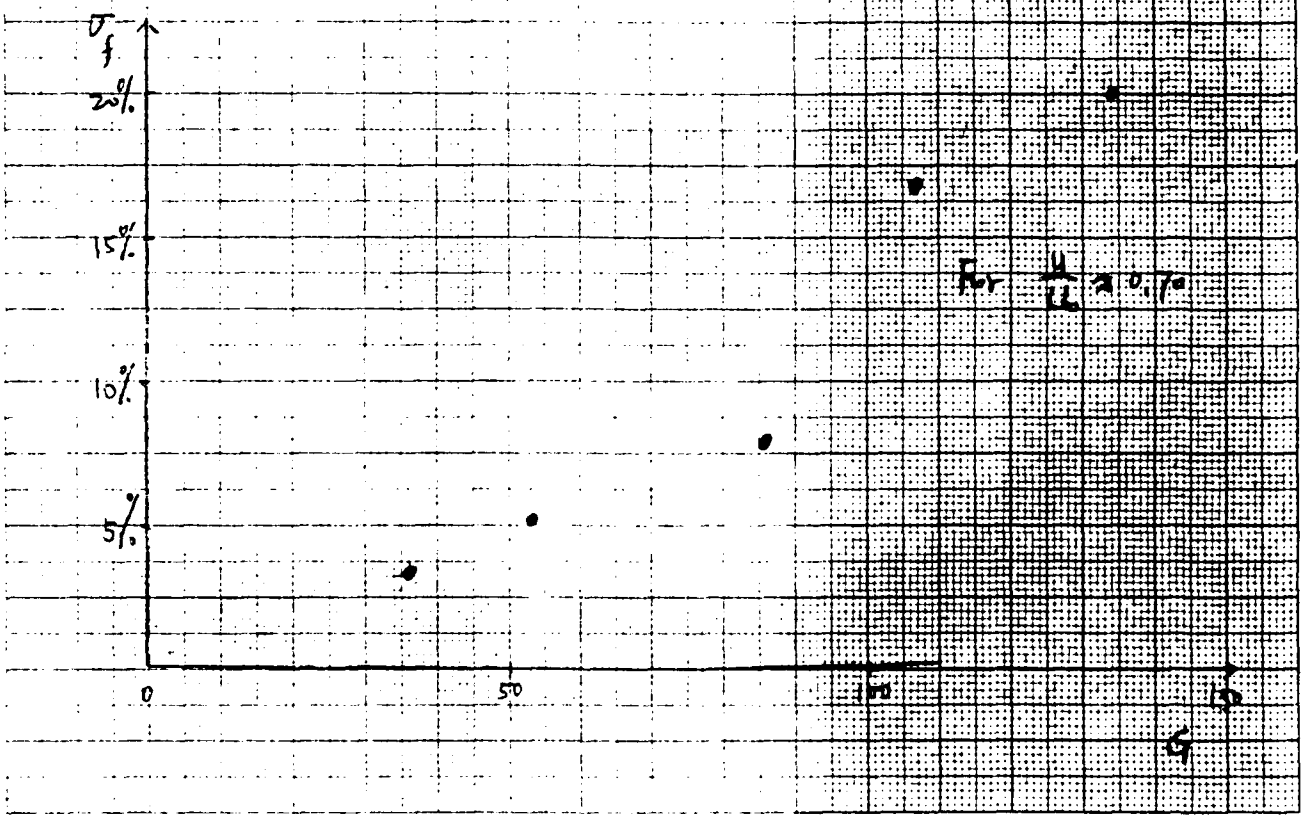

Fig. 13 Variation of Velocity Disturbance Level

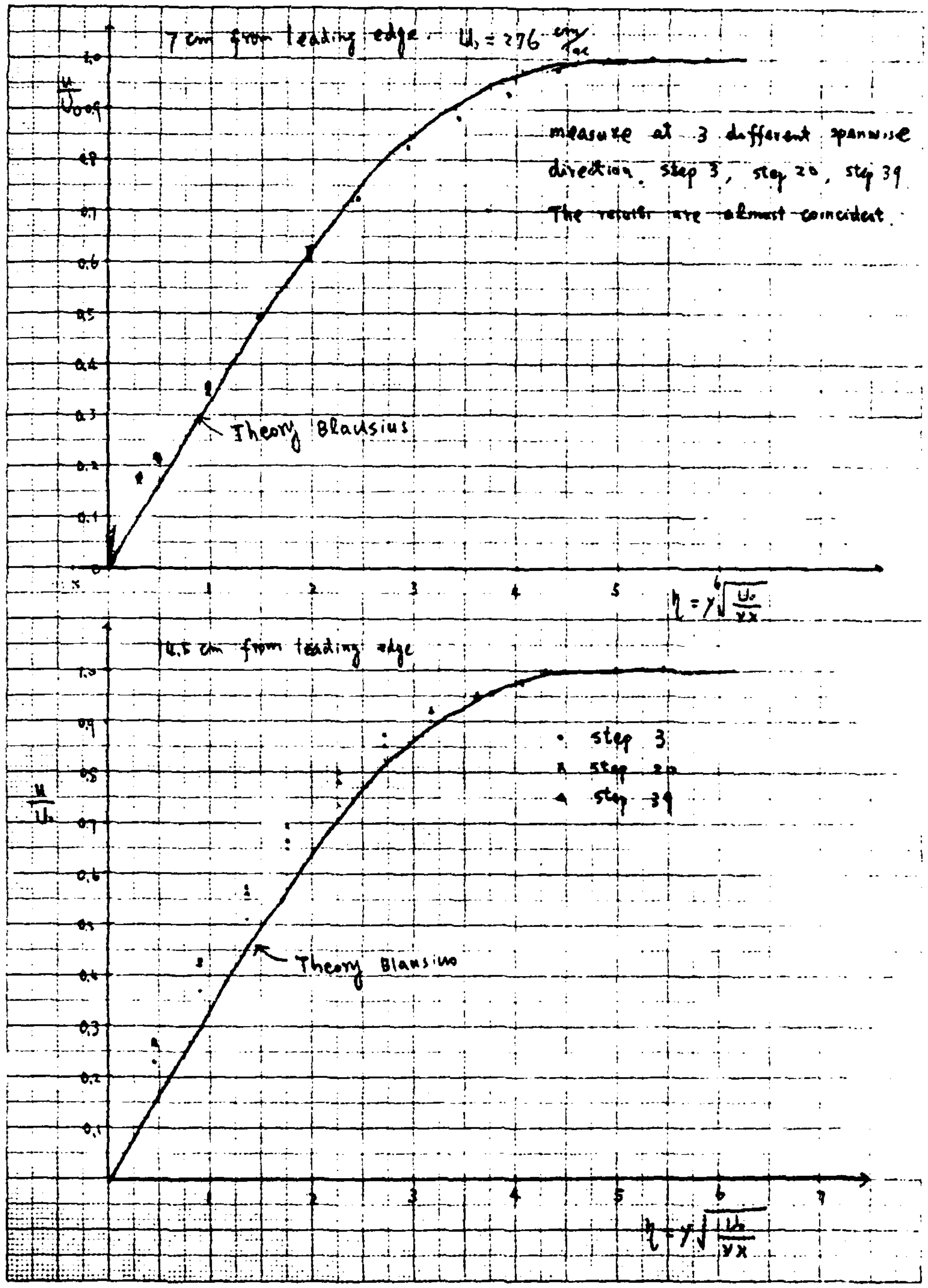

Fig 14 Boundary Layer Velocity Profile

461510

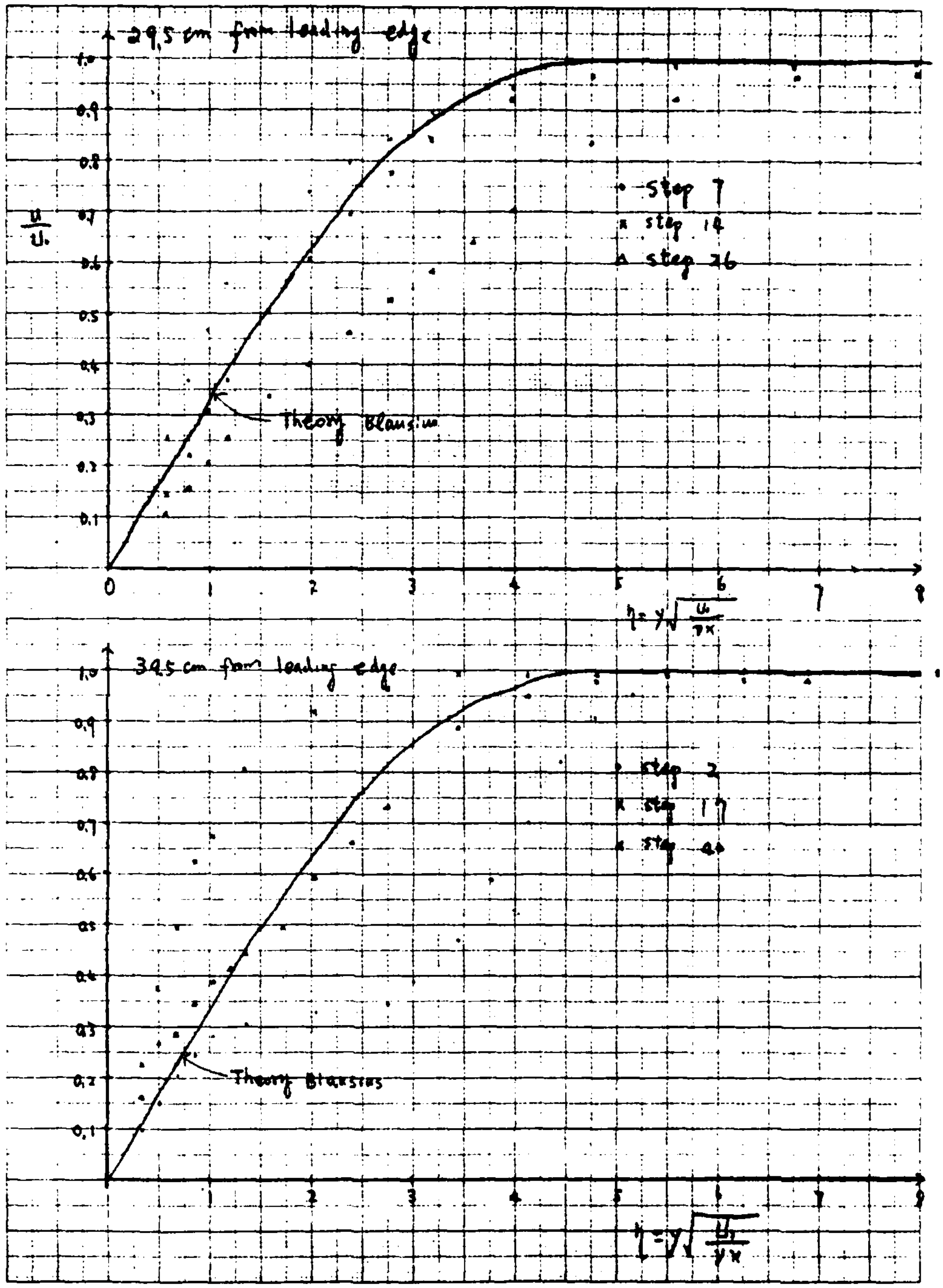

Fig. 15 Boundary Layer Velocity Profile